Order-disorder effects on the equation of state for fcc Ni-Al alloys

H. Y. Geng,[1,2] M. H. F. Sluiter,[3] and N. X. Chen[1,4]
[1]*Department of Physics, Tsinghua University, Beijing 100084, China*
[2]*Laboratory for Shock Wave and Detonation Physics Research, Southwest Institute of Fluid Physics, P.O. Box 919-102, Mianyang Sichuan 621900, China*
[3]*Institute for Materials Research, Tohoku University, Sendai, 980-8577 Japan*
[4]*Institute for Applied Physics, University of Science and Technology, Beijing 100083, China*
(Received 21 February 2005; revised manuscript received 3 May 2005; published 18 July 2005)

Order-disorder effects on equation of state (EOS) properties of substitutional binary alloys are investigated with the cluster variation method (CVM) based on *ab initio* effective cluster interactions (ECI). Calculations are applied to the fcc based system. Various related quantities are shown to vary with concentration around stoichiometry with a surprising "W shape," such as the thermal expansion coefficient, the heat capacity, and the Grüneisen parameter, due to configurational ordering effects. Analysis shows that this feature originates from the dominated behavior of some elements of the inverse of Hessian matrix, and relates to antisite defects occurring around stoichiometric compositions. This kind of strong compositional effects on EOS properties highlights the importance of subtle thermodynamic behavior of order-disorder systems.

DOI: 10.1103/PhysRevB.72.014204 PACS number(s): 64.30.+t, 64.60.Cn, 65.40.−b, 61.66.Dk

I. INTRODUCTION

The equation of state (EOS) is a primary but important property to understand materials behavior. Although the theory of the EOS for elemental substances is well-developed in both the ordinary density[1,2] and the abnormal density region,[3,4] its extension to alloys and compounds is a rather recent development[5] and some interesting results have been obtained.[6] It has been understood that ordering and disordering process have considerable effects on phase stability and thermodynamic behaviors of materials, as well as on the EOS, of course. For example, the pressure is increased considerably due to the order-disorder transition along the Hugoniot in Ni_3Al.[6] However, this effect on the EOS was investigated only at constant composition. Initial calculations have pointed to surprising compositional variations in the heat capacity.[7,8] Though these calculations dealt with simple models and some important contributions were ignored, a theoretical analysis showed that the so-called "W shape" of heat capacity around stoichiometric compositions is a general feature of ordered alloys[9] and similar phenomena can be expected for other thermodynamic quantities.

First-principles calculations based on density functional theory (DFT) have received much attention for the study of alloy phase stability with contributions from chemical effects[10] and lattice vibrations.[11] For the EOS, first-principles results are not as accurate as might be expected,[12] mainly because of the large error in calculating the bulk modulus of transition metals and the difficulty to accurately account for lattice vibrations and local distortions. However, the precision of current *ab initio* results is high enough for making definite predictions, and will be employed in this work to derive effective cluster interactions (ECI).

For a full understanding of the properties of alloys, knowledge of formation free energy alone is not completely sufficient. The information of the EOS is essential for understanding mechanical and thermodynamical properties during adiabatic compression and so on. Thus all Gibbs free energy contributions must be considered.[5] A combination of the cluster expansion method (CEM) and the cluster variation method (CVM) provides a natural and feasible approach to evaluate the EOS of alloys and solid solutions, in which configurational effects are included explicitly. The effects of ordering and disordering process can be modelled directly in this framework by variation principle of minimizing Gibbs function with respect to volume and correlation functions. It is necessary to point out that unlike vibrational and electronic excitations, excitations associated with short or long ranged order have large energy barriers so that nonequilibrium states are easily reached. Therefore, it is quite suitable to separate out the effect of ordering on the thermal properties.

In this paper we calculate order-disorder effects on the EOS and related thermal quantities for binary fcc Ni-Al alloys using *ab initio* chemical and lattice vibrational contributions. The methodology of our calculations is discussed briefly in the next section. The model to approximate the contribution of lattice vibrations is described and ordering corrections to the thermal expansion coefficient, heat capacity at constant pressure, Grüneisen parameter and so forth are derived and calculated. The implications of the strong composition dependence are discussed.

II. METHODOLOGY

For substitutional binary alloys, the Gibbs free energy can be written as

$$\hat{G} = \sum_i \left[[v_i(V) + w_i(V,T)] \cdot \xi_i + k_B T \times \sum_{\alpha_i} a_{\alpha_i} \mathrm{Tr}_{\alpha_i} \rho_{\alpha_i} \log \rho_{\alpha_i} + PV \right], \quad (1)$$

where the summation is over all types of clusters, a_{α_i} is the möbius inversion coefficient of cluster α_i of type i which

satisfies $a_{\alpha_i}=\Sigma'_{\beta\supset\alpha_i}(-1)^{|\beta/\alpha_i|}$, the prime indicates the summation is restricted by maximal clusters; ρ_{α_i} is the density matrix of cluster α_i and is related to correlation functions ξ_i by

$$\rho_{\alpha_i}=\rho^0_{\alpha_i}\left(1+\sum_{\substack{\beta_j\subset\alpha_i\\ \beta_j\neq\emptyset}}\xi_j\sigma_{\beta_j}\right),\quad \rho^0_{\alpha_i}=2^{-|\alpha_i|}.$$

Here σ_{β_j} is the cluster occupation variable and $|\alpha_i|$ is the number of sites contained in the α_i cluster.[13] The chemical and vibrational effective cluster interactions (ECI) $v_i(V)$ and $w_i(V,T)$ are derived by a generalized Connolly-Williams procedure[14] with cohesive energies and vibrational free energies of a set of superstructures,

$$v_i(V)=\sum_S(\xi_i^S)^{-1}E^S(V), \tag{2}$$

$$w_i(V,T)=\sum_S(\xi_i^S)^{-1}F_v^S(V,T). \tag{3}$$

The superscript S denotes the superstructures and $(\xi_i^S)^{-1}$ is the general pseudo-inverse, i.e., the Moore-Penrose inverse of the correlation function matrix, which gives the least squares solution for overdetermined systems of equations.[15]

The vibrational free energy of each superstructure is described approximately by Debye-Grüneisen (MJS) model[16]

$$F_v(V,T)=3k_BT\ln(1-\exp(-\Theta_D/T))-k_BTD(\Theta_D/T)+\frac{9}{8}k_B\Theta_D, \tag{4}$$

where k_B is Boltzmann's constant and D is the Debye function. The Debye temperature is approximated as[16]

$$\Theta_D=[c\cdot d_{\mathrm{Al}}+(1-c)\cdot d_{\mathrm{Ni}}]\left[\frac{BV^{1/3}}{M}\right]^{1/2}, \tag{5}$$

where B is the bulk modulus as determined from the cohesive energy curve, M is the atomic weight, and c is the concentration of Al. Scaling factors d_{Al} and d_{Ni} are determined from experimental Θ_D's of constituent elements at ambient condition, respectively (423 K for Al and 427 K for Ni), to remedy this model for transition metals and their alloys. One should be noticed that the linear prefactor in Eq. (5) is just a semiempirical way to improve the agreement between calculated and measured Debye temperatures for the pure elements. The Debye temperature still depends in a nontrivial way on the state of order in the alloy through the bulk modulus B and the atomic volume V. It is necessary to point out that the Debye-Grüneisen model is a little crude. It does not have the capability to model the phonon density of state (DOS) at high frequencies properly, which results in inaccurate vibrational entropy difference among phases. However, this is not so serious because the contribution from the vibrational energy becomes more important than entropy for EOS calculations and the Grüneisen parameter is dependent mainly on low frequencies part of phonon DOS. A much more severe limitation of this model is that for cluster expansion procedure Eq. (5) sometimes will become ill-defined, even breaks down completely when the atomic volume is beyond the inflection point of the cohesive energy curve where the bulk modulus $B=0$. Ni-Al alloys exemplify this case, where at the Al-rich region, the equilibrium volume is beyond the inflection point of the Ni cohesive energy and the bulk modulus and Debye temperature cannot be defined properly. Therefore, in order to use the Debye-Grüneisen model, a certain hydrostatic pressure must be applied to reduce the size difference between Ni and Al. In this paper, a pressure of 30 GPa is used.

The equilibrium Gibbs function is obtained by the variational principle

$$G=\hat{G}|_{\partial\hat{G}/\partial\xi_i=\partial\hat{G}/\partial V=0}. \tag{6}$$

Then the EOS and other related quantities can be derived directly. In the framework of CVM+CEM, these quantities are calculated by numerical differentiation. For example, the thermal expansion coefficient at composition c, temperature T_0, and pressure P_0 is evaluated using the formula

$$\alpha(c,T_0,P_0)=\frac{1}{V(c,T_0,P_0)}\left[\frac{V(c,T_0+\Delta T,P_0)-V(c,T_0-\Delta T,P_0)}{2\Delta T}\right]. \tag{7}$$

Other quantities, the compressibility κ, heat capacity at constant pressure C_P and isobaric EOS parameter R[3,4] can be calculated analogously with

$$\kappa=-\frac{1}{V}\left(\frac{\partial V}{\partial P}\right)_T, \tag{8}$$

$$C_P=\left(\frac{dH}{dT}\right)_P, \tag{9}$$

$$R=\frac{P}{C_P}\left(\frac{\partial V}{\partial T}\right)_P. \tag{10}$$

The isochoric EOS parameter (i.e., Grüneisen parameter) γ, and the coefficient of pressure β, however, must be computed indirectly via other thermal quantities because it is impossible to fix volume when the equilibrium Gibbs free energy is obtained variationally. Generally, the Grüneisen parameter can be obtained with

$$\gamma=\frac{\alpha V}{\kappa C_V}, \tag{11}$$

where the heat capacity at constant volume is given by $C_V=C_P-TPV\alpha\beta$ and the coefficient of pressure $\beta=\alpha/P\kappa$.

III. CALCULATIONS AND DISCUSSIONS

A. *Ab initio* calculations and phase diagram

Cohesive energies of some hypothetical Ni-Al fcc-based superstructures have been listed in Ref. 5. Here the cohesive energies of some additional structures are given as computed with CASTEP (Refs. 17 and 18) with the generalized gradient approximation (GGA) (Ref. 19) for fcc lattice parameters

TABLE I. Cohesive energies of fcc superstructures at 0 GPa.

Structure	c_{Al}	E_{coh} (eV/atom)	a (Å)
$C2/m$	0.333	−4.779	3.578
$MoPt_2$	0.333	−4.725	3.588
$L1_1$	0.5	−4.412	3.681
$Z2$	0.5	−4.232	3.703
$NR40$	0.5	−4.617	3.652
$C2/m$	0.667	−4.203	3.770
$MoPt_2$	0.667	−4.224	3.768

from 2.8 to 4.8 Å. The calculations employ ultrasoft pseudopotentials[20] with a cutoff kinetic energy for plane waves of 540 eV. Integrations in reciprocal space are performed in the first Brillouin zone with a k-point grid with a maximal interval of 0.03 $Å^{-1}$ as generated with the Monkhorst-Pack[21] scheme. The energy tolerance for the charge self-consistency convergence is 2 μeV/atom for all calculations. Cohesive energies at different lattice parameters are extracted from the total energies by subtracting the spin-polarized energies of isolated atoms. Then, they are fitted to Morse-type energy functions which are used to derive ECIs.

The calculated equilibrium lattice parameters and cohesive energies at zero pressure are listed in Table I. NR40 and $C2/m$ are the most stable structures. We have tried to calculate the ground states and phase diagram at finite temperature with CEM and CVM approach[13,22,23] with the tetrahedron-octahedron (T-O) approximation by inclusion of these new structures with those listed in Table II of Ref. 5. However, it fails due to the relative order of stability of superstructures is modified by the CEM procedure. Although the use of the T-O approximation could, in principle, improve the accuracy of the results, we found that an accurate fit of a cluster expansion within the T-O approximation that correctly reproduces the ground states would have required a much larger number of input structures. The T-approximation, however, was found to be able to reproduce the known ground states in the studied systems, thus capturing their qualitative behavior, which is enough for the purpose of this work.

After excluding the $Z2$ and $C2/m$ (Ni_4Al_2) structures from above mentioned superstructures, a set of ECIs (Ref. 24) is derived within the T-approximation (using 12 superstructures) that faithfully produces the correct ground states. The corresponding phase diagrams at a hydrostatic pressure of 30 GPa are plotted in Fig. 1, where horizontal lines indicate the temperatures at which the configurational corrections of the EOS properties have been calculated as functions of composition. Here global relaxation (for the elastic energy partially) is taken into account, which is responsible for the phase separation at the Al-rich side; and hydrostatic pressure is implemented to reduce the size difference between Ni and Al so that the CEM bulk modulus of the pure phases is well defined. For comparison, the phase diagram without vibrational contribution is presented also. It is seen that order-disorder transition temperatures of $L1_2$ and $L1_0$ are slightly lowered by vibrational contributions, but less than 100 K.

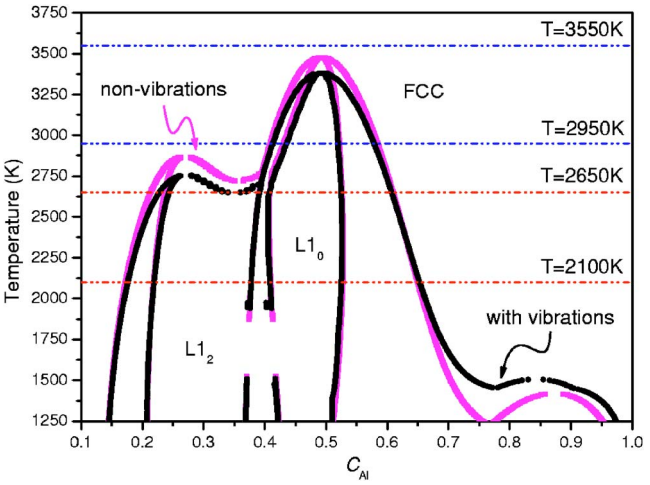

FIG. 1. (Color online) The phase diagram of fcc Ni—Al in the T approximation with elastic relaxations included. For comparison, both with and without vibrational effects are shown.

Considering that including vibrations through anharmonicity causes a volume expansion, it appears that in actuality the effect of vibrations on the order-disorder temperatures is even less. Therefore, vibrational effects on phase diagram of fcc Ni-Al appear very minor, in agreement with that inferred from first-principles calculations of the vibrational entropy.[25] However, when bcc-based structures are included, this statement might have to be reconsidered.[26]

B. Order-disorder effects on EOS quantities

Generally, thermal expansion of materials originates from anharmonic lattice vibrations. However, in the case of alloys, configurational effects are another source of thermal expansion, although its magnitude is not as large as that of vibrations. Figure 2 shows the configurational excess thermal expansion coefficient α, computed at fixed temperatures of

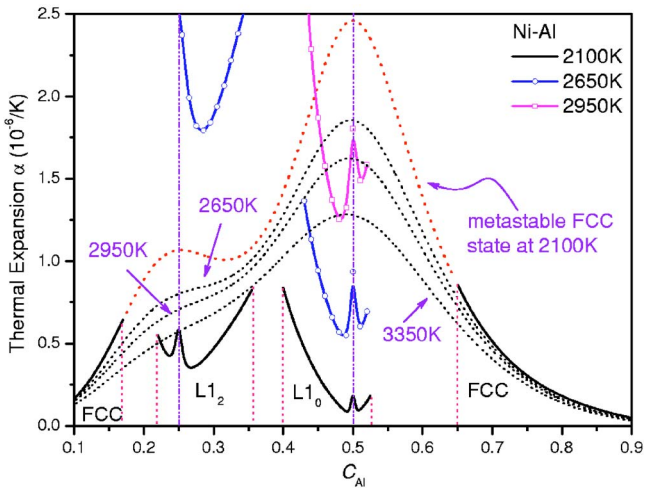

FIG. 2. (Color online) Thermal expansion coefficient of Ni-Al alloys without vibrational contributions as a function of composition. Solid lines are for single phases and dotted curves are for metastable/coexisting disordered phases.

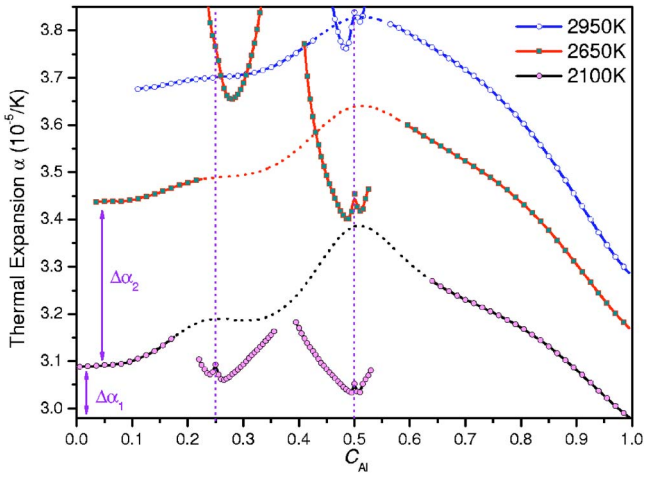

FIG. 3. (Color online) Thermal expansion coefficient of Ni-Al alloys with vibrational contributions at different temperatures. The dotted lines denote the metastable/coexisting region of the disordered phase.

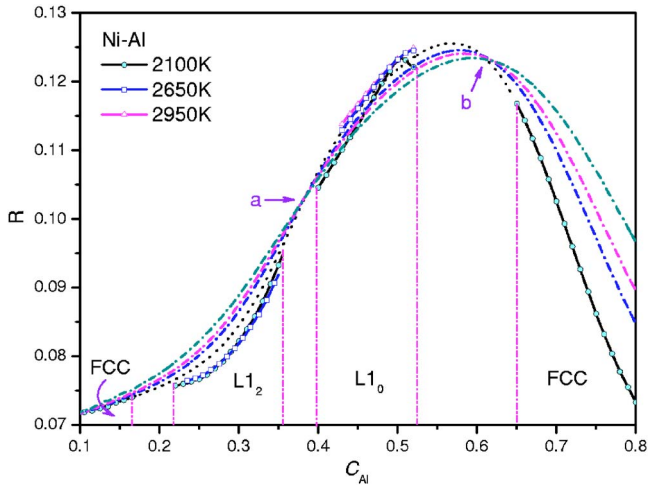

FIG. 4. (Color online) Isobaric EOS parameter R as a function of Al concentration, without vibrational contributions. Dashed-dotted lines indicate those of the fcc phase at 2650, 2950, and 3550 K, respectively.

2100, 2650, 2950, and 3350 K, respectively, as indicated in Fig. 1. Stable and unstable phases and two phase regions can be found easily from Fig. 1. It is evident that for the metastable fcc phase, increasing temperature always decreases α, reflecting the loss of short range order. This might suggest that ordering increases α. However, for stable ordered phases ($L1_2$ and $L1_0$), α increases with temperature. This apparent contrast can be understood when realizing that disordering in the ordered state accelerates as the temperature increases. Some other details are particular interesting. The most noticeable features are the peaks and wings around stoichiometric compositions. According to Sluiter and Kawazoe[9] this is due to antisite defects near stoichiometry. The second remarkable feature is that at low temperatures, α of the ordered phase is much smaller than that of the fcc phase. However, when the temperature approaches the order-disorder transition temperature T_c, α in the ordered state rapidly increases and greatly exceeds the disordered α. This leads to a sharp drop in α at T_c when order-disorder transition is completed. Actually, according to Eq. (7) and the fact that order-disorder transitions on fcc lattice are always first order, which results in a jump of volume at T_c, we can conclude that α diverges at T_c and has a steeper drop on disorder side. The same conclusion is also valid for heat capacity, but not for compressibility, since pressure also jumps at T_c and with Eq. (8) the compressibility has a finite value at T_c.

These observations still are valid when vibrational contributions are included, as is shown in Fig. 3. Including vibrations now lead to α of the disordered phase that consistently increases with temperature. The α curves also become more smooth with increasing temperature. The difference between α of the ordered and disordered phases is enhanced a little by lattice vibrations. Simultaneously, the peaks near stoichiometric compositions become less pronounced than those in Fig. 2. In Fig. 3, $\Delta\alpha_1$ is the difference between the α of Ni and that of Al at 2100 K, and $\Delta\alpha_2$ is the increment of α of Ni when temperature raised from 2100 K to 2650 K. It is seen that their values are not so large and are comparable with the difference of α between ordered and disordered phases. This kind of variation of α (curves in Fig. 3) as a function of composition and temperature due to ordering/disordering process has not been reported before. Considering that actual materials generally are not perfectly single phases with homogeneous composition, the strong composition dependence of the thermal expansion coefficient might contribute to thermal stresses in alloys (the same conclusion is also valid for mineral crystals).

The EOS parameter R (for isobaric) and γ (Grüneisen parameter, for isochoric) are also modified by configurational corrections. The variation of the former with Al concentration is plotted in Fig. 4. The Grüneisen parameter has a shape very similar to the EOS parameter R when vibrational contributions are excluded. It is evident that the effect of short-range ordering is very strong. In contrast, long-range ordering corrections are very limited, just a slightly lower (higher) R in the $L1_2$ ($L1_0$) single phase region.

Remarkably, there are two points (a and b in Fig. 4) where R appears constant with temperature for the metastable fcc phase at both sides of the $L1_0$ phase. However, these points do not occur when lattice vibrations are included and we believe they have little significance for materials behavior.

When lattice vibrations are taken into account the behavior of the isochoric and isobaric EOS parameters changes significantly. Figure 5 shows the isochoric EOS parameter as a function of the Al concentration at different temperatures. The cross points a and b in Fig. 4 are removed by vibrational effects. The upset "W-shape" (pointed out by arrow) appears near stoichiometry. Although γ of the $L1_0$ is rather temperature independent, γ of the $L1_2$ phase is not. This is probably due to the order-disorder transformation of the $L1_2$ phase in the displayed temperature range. Above the order-disorder temperature γ attains a higher value again, as the 2950 K data shows (line c in Fig. 5). This kind of rapid change of the Grüneisen parameter explains the sudden increase in pressure during an order-disorder transition in Ni_3Al.[6]

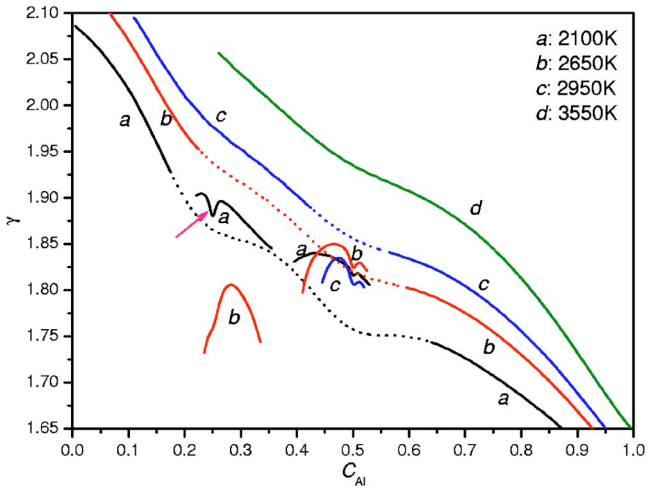

FIG. 5. (Color online) The Grüneisen parameter as a function of Al concentration at different temperatures. Vibrational contributions are included.

The heat capacity at constant pressure C_P has a very similar shape as that of the thermal expansion coefficient. It suggests there is a common underlying cause. The variation of C_P with Al concentration and temperature is shown in Fig. 6.[27] Its variation with concentration (including the peaks and wings) and with temperature is considerable, which would enhance the inhomogeneous temperature distribution during heat treatments of alloys.

The compressibility κ is an important property to model compression behavior of materials under high pressures. It is related to the bulk sound velocity via a simple thermodynamic relation. Order/disorder process has little effect on κ. It is slightly lower in the ordered phases than in the disordered fcc phase, as shown in Fig. 7. Thus, long-range order has little influence on the bulk sound velocity. However, a deviation from linearity due to short-range order is apparent. For the bcc lattice, it must be pointed out that the situation is somewhat different. We have in fact observed that both

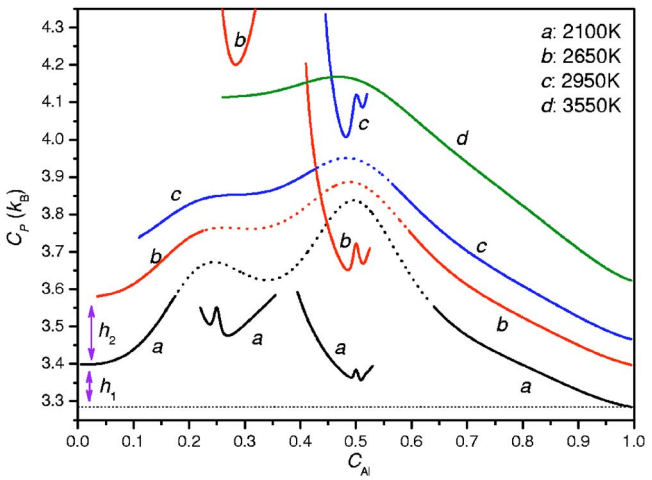

FIG. 6. (Color online) The heat capacity at a constant pressure of 30 GPa for Ni-Al alloys with vibrational contributions included. Notice the similarity with the thermal expansion coefficient.

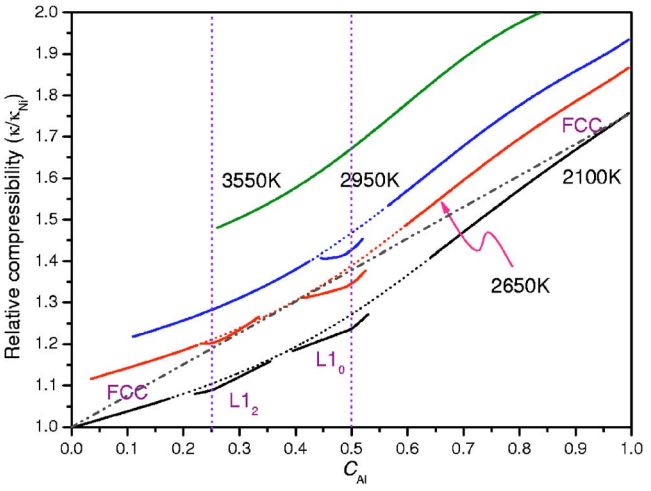

FIG. 7. (Color online) The compressibility at 30 GPa of Ni-Al alloys with vibrational contributions included. The dashed-dotted-dotted line indicates the linear interpolation. For the mechanical mixture model κ is slightly upwards protruding.

strong short- and long-range order effects are presented there, whereas the "W-shape" is still absent (not shown here).

To better understand the behavior of alloys mentioned above, it is helpful to decompose the Gibbs free energy of formation into contributions such as internal energy, vibrational entropy, configurational entropy and volume difference times pressure, respectively. The formation Gibbs free energy is defined relative to that of the mixing model, namely, the mechanical mixture of the ingredients as

$$\Delta G(T,P) = G - [c_{\mathrm{Al}}G_{\mathrm{Al}}(T,P) + (1-c_{\mathrm{Al}})G_{\mathrm{Ni}}]$$
$$= \Delta E + P\Delta V - T\Delta S_{\mathrm{vib}} - TS_{\mathrm{cvm}}. \qquad (12)$$

The magnitudes of each partial Gibbs free energy of formation at 2100 K and 30 GPa are shown in Fig. 8. The internal

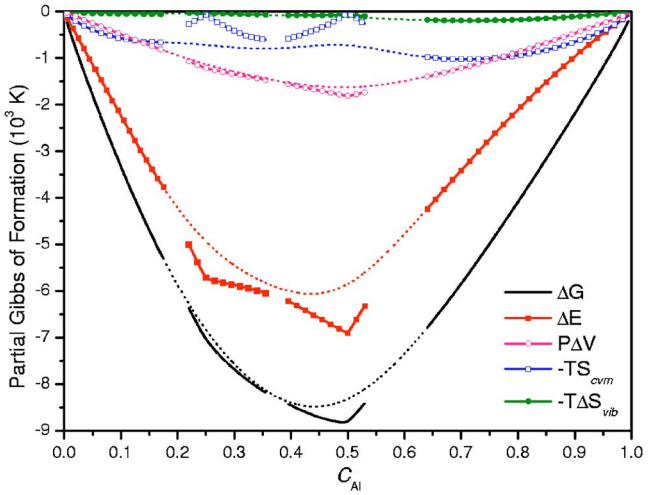

FIG. 8. (Color online) The partial Gibbs free energy of formation at 30 GPa and 2100 K for the fcc Ni-Al system. Dotted lines indicate metastable/coexisting phase regions.

energy is the largest contribution, followed by the volume difference and configurational entropy terms. The vibrational entropy difference is much less and almost negligible. The sharp turns in the curves of internal energy and configurational entropy in the ordered single phase region suggest a connection to the "W-shape" of the EOS properties.

Variations of the EOS quantities as functions of temperature, pressure, and concentration are determined completely by the Gibbs free energy as a functional of volume V and correlation functions ξ_i (after integrating out other degrees of freedom, say, the concentration c). By defining a vector variable $\eta_0=V$ and $\eta_i=\xi_i$, $(i=1,2,\ldots)$, and using the variational condition $\delta G/\delta\eta=0$, one obtains

$$\left(\frac{\partial\eta}{\partial T}\right)_i = \sum_j \left(\frac{\partial^2 G}{\partial\eta\partial\eta}\right)^{-1}_{i,j}\left[\frac{\partial H}{T\partial\eta} - \frac{\partial^2 H}{\partial T\partial\eta} + T\frac{\partial^2 S}{\partial T\partial\eta}\right]_j, \quad (i,j=0,1,2,\ldots), \tag{13}$$

where H is enthalpy and S the entropy including vibrational contributions. $(\partial^2 G/\partial\eta\partial\eta)^{-1}$ is the inverse of the Hessian matrix with subscripts i and j labeling matrix elements. Using this relation, the heat capacity C_P is given by

$$\begin{aligned} C_P &= \left(\frac{dH}{dT}\right)_{c,P} = \frac{\partial H}{\partial T} + \sum_i \left(\frac{\partial H}{\partial\eta_i}\right)_{c,P}\left(\frac{\partial\eta_i}{\partial T}\right)_{c,P} \\ &= \frac{\partial H}{\partial T} + \sum_{ij}\left(\frac{\partial H}{\partial\eta}\right)_i\left(\frac{\partial^2 G}{\partial\eta\partial\eta}\right)^{-1}_{i,j} \\ &\quad\times\left[\frac{\partial H}{T\partial\eta} - \frac{\partial^2 H}{\partial T\partial\eta} + T\frac{\partial^2 S}{\partial T\partial\eta}\right]_j. \end{aligned} \tag{14}$$

Here the subscripts c, P indicate that both composition c and pressure P are constants. Similarly, the thermal expansion coefficient α is expressed as

$$\alpha = \frac{1}{V}\left(\frac{\partial V}{\partial T}\right)_P = \frac{1}{V}\sum_i \left(\frac{\partial^2 G}{\partial\eta\partial\eta}\right)^{-1}_{0,i}\left[\frac{\partial H}{T\partial\eta} - \frac{\partial^2 H}{\partial T\partial\eta} + T\frac{\partial^2 S}{\partial T\partial\eta}\right]_i, \tag{15}$$

and Grüneisen parameter γ is related to the correlation functions via Eq. (11) where the heat capacity at constant volume C_V is given by

$$\begin{aligned} C_V &= \left(\frac{dE}{dT}\right)_{c,V} = \frac{\partial E}{\partial T} + \sum_{ij}\left(\frac{\partial E}{\partial\xi}\right)_i\left(\frac{\partial^2 F}{\partial\xi\partial\xi}\right)^{-1}_{i,j} \\ &\quad\times\left[\frac{\partial E}{T\partial\xi} - \frac{\partial^2 E}{\partial T\partial\xi} + T\frac{\partial^2 S}{\partial T\partial\xi}\right]_j, \end{aligned} \tag{16}$$

where F is the Helmholtz free energy and E the internal energy. These relations indicate that the "W-shape" is directly related to the behavior of inverse Hessian matrix. Some of its elements dominate the detailed thermodynamical behavior of alloys, mainly from the variation of Gibbs free energy with respect to correlation functions.[28] In contrast to the previously mentioned properties, the compressibility is determined only by the variation of free energy with respect to volume

$$\kappa^{-1} = V\frac{\partial^2 F}{\partial V^2}. \tag{17}$$

It is unrelated to any correlation functions, and then the "W-shape" is also absent, as shown in Fig. 7, so as for the bulk sound velocity on bcc-based phases. As the "W-shape" composition dependence is governed mainly by the general behavior of the inverse of Hessian matrix with respect to correlation functions for order-disorder systems, the conclusions drawn here should be valid also for other system, e.g., interstitial alloys and mineral crystals.

IV. CONCLUSION

The variation of EOS quantities as functions of concentration and temperature as calculated with *ab initio* ECIs was presented. The "W-shape" in the composition dependence around stoichiometry is observed for several important properties. Analysis shows that this kind of behavior is related to the behavior of the inverse of Hessian matrix with respect to correlation functions. This explains the similarity in behavior of the heat capacity and the thermal expansion coefficient, and the absence of the "W-shape" near stoichiometry for the compressibility and the bulk sound velocity. The strong composition dependence near stoichiometry due to configurational corrections has not received much attention before and may be helpful for understanding subtle phenomena in alloys and mineral crystals. The configurational corrected Grüneisen parameter is also shown to have strong composition dependence near stoichiometry around T_c. This suggests that the EOS of order-disorder systems is much more complicated than previously expected and that configurational effects cannot be neglected.

ACKNOWLEDGMENTS

This work was supported by the National Advanced Materials Committee of China. The authors gratefully acknowledge the financial support from 973 Project in China under Grant No. G2000067101. Part of this work was performed under the interuniversity cooperative research program of the Laboratory for Advanced Materials, Institute for Materials Research, Tohoku University.

[1] S. Eliezer, A. Ghatak, and H. Hora, *An Introduction to Equation of State: Theory and Applications* (Cambridge University Press, Cambridge, 1986).

[2] X. Xu and W. Zhang, *Theoretical Introduction to Equation of State* (Science Press, Beijing, 1986) (in Chinese).

[3] H. Y. Geng, Q. Wu, H. Tan, L. C. Cai, and F. Q. Jing, J. Appl. Phys. **92**, 5917 (2002); Q. Wu and F. Q. Jing, *ibid.* **80**, 4343 (1996).

[4] H. Y. Geng, Q. Wu, H. Tan, L. C. Cai, and F. Q. Jing, J. Appl. Phys. **92**, 5924 (2002).
[5] H. Y. Geng, N. X. Chen, and M. H. F. Sluiter, Phys. Rev. B **70**, 094203 (2004).
[6] H. Y. Geng, N. X. Chen, and M. H. F. Sluiter, Phys. Rev. B **71**, 012105 (2005).
[7] C. G. Schön and G. Inden, Acta Mater. **46**, 4219 (1998).
[8] A. Kusoffsky and B. Sundman, J. Phys. Chem. Solids **59**, 1549 (1998).
[9] M. Sluiter and Y. Kawazoe, Phys. Rev. B **59**, 3280 (1999).
[10] M. H. F. Sluiter, Y. Watanabe, D. de Fontaine, and Y. Kawazoe, Phys. Rev. B **53**, 6137 (1996).
[11] A. van de Walle and G. Ceder, Rev. Mod. Phys. **74**, 11 (2002).
[12] C. W. Greeff and M. J. Graf, Phys. Rev. B **69**, 054107 (2004).
[13] F. Ducastelle, *Order and Phase Stability in Alloys* (Elsevier Science, New York, 1991).
[14] J. W. D. Connolly and A. R. Williams, Phys. Rev. B **27**, 5169 (1983).
[15] For EOS calculations, since relative stability of superstructures depends on temperature and atomic volume, it is difficult to employ improved CW procedures [see Ref. 10 and G. D. Garbulsky and G. Ceder, Phys. Rev. B **51**, 67 (1995)] and it seems that the pseudo-inverse is the best approach to obtain ECIs.
[16] V. L. Moruzzi, J. F. Janak, and K. Schwarz, Phys. Rev. B **37**, 790 (1988). Here a few modifications have been adopted to improve this model for transition and weak magnetic alloys.
[17] Accelrys Inc., CASTEP Users Guide (Accelrys Inc., San Diego, 2001).
[18] V. Milman, B. Winkler, J. A. White, C. J. Pickard, M. C. Payne, E. V. Akhmatskaya, and R. H. Nobes, Int. J. Quantum Chem. **77**, 895 (2000).
[19] J. P. Perdew, K. Burke, and M. Ernzerhof, Phys. Rev. Lett. **77**, 3865 (1996).
[20] D. Vanderbilt, Phys. Rev. B **41**, R7892 (1990).
[21] H. J. Monkhorst and J. D. Pack, Phys. Rev. B **13**, 5188 (1976).
[22] D. de Fontaine, in *Solid State Physics*, edited by H. Ehrenreich and D. Turnbull (Academic, New York, 1994), Vol. 47, p. 84.
[23] A. Pasturel, C. Colinet, A. T. Paxton, and M. van Schilfgaarde, J. Phys.: Condens. Matter **4**, 945 (1992).
[24] This is the main shortcoming of CEM that it cannot always guarantee the improvement of the quality of ECI with increasing maximal clusters and including more superstructures, as pointed out in M. Sluiter and P. E. A. Tuichi, Phys. Rev. B **40**, 11215 (1989). To ensure the relative stability of phases not be changed by CEM, some special techniques are required. However, as mentioned in Ref. 15, it is difficult to implement them for EOS calculations.
[25] A. van de Walle, G. Ceder, and U. V. Waghmare, Phys. Rev. Lett. **80**, 4911 (1998).
[26] J. R. Soh and H. M. Lee, Acta Mater. **45**, 4743 (1997).
[27] The variation of the heat capacity at constant volume is imaginable based on this figure for pure elements obeyed by Dulong-Petit's Law and its shape is actually analogous to Fig. 2. Therefore it is not shown here.
[28] Generally speaking, various ordering/disordering effects are related to the variation of configurational entropy. Since a necessary condition for the occurrence of antisite defects is that for a small but finite variation of ξ away from the perfect site occupations, one must have $\Delta H/\Delta\xi - T\Delta S_{\mathrm{cvm}}/\Delta\xi < 0$ (here the vibrational entropy has been ignored due to Fig. 8); it is evident that temperature activates antisite defects. On the other hand, the variation of correlation functions is given by $\Delta\xi_i = -\Sigma_j(\partial^2 G/\partial\eta\partial\eta)^{-1}_{i,j}(\partial G/\partial\eta)_j$. In this way, the configurational entropy effects are transferred to the inverse of the Hessian matrix via $\Delta\xi$, and then to $(\partial V/\partial T)_P$, which is proportional to $(\partial^2 G/\partial\eta\partial\eta)^{-1}_{0,i}$. In this sense, all kinds of "W-shape" arise from the composition dependent behavior of $\partial\eta_i/\partial T$, which all relate to $\partial^2 S_{\mathrm{cvm}}/\partial\xi_i\partial\xi_j$ (that has a "W shape" behavior along composition axis, see Ref. 9) through the inverse of the Hessian matrix.